

Effects of iron on greenhouse gases and ammonia emissions and related genes in swine manure composting

Chen Zhang ^{a,b}, Xi Chen ^c, Hailong Mao ^b, Xiuming Zhang ^d, Ke Wang ^{a,b,*}, Enhao Zhu ^b, Dan Yin ^b, Ruilun Zheng ^{e,**}, Shijie You ^b

^a National Engineering Research Center for Safe Sludge Disposal and Resource Recovery, Harbin Institute of Technology, Harbin, 150090, China

^b State Key Laboratory of Urban-rural Water Resource and Environment, School of Environment, Harbin Institute of Technology, Harbin, 150090, China

^c Changchun University of Architecture and Civil Engineering, Changchun, 130607, China

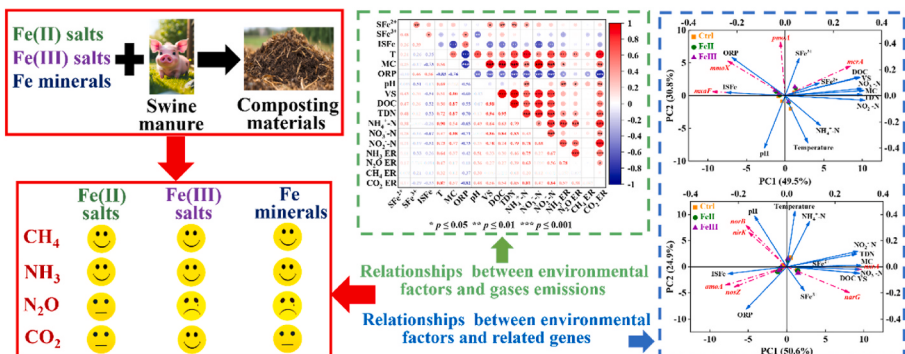
^d Grandblue (Harbin) Biological Technology Co., Ltd, Harbin, 150040, China

^e Institute of Grassland, Flowers and Ecology, Beijing Academy of Agriculture and Forestry Sciences, Beijing, 100097, China

HIGHLIGHTS

- Effects of five Fe salts and five Fe minerals on GHGs and NH₃ were evaluated.
- Fe(III) salts were superior to Fe(II) salts and Fe minerals on reducing CO₂, CH₄, NH₃.
- Fe(III) salts and Fe minerals promoted more N₂O emission relative to Fe(II) salts.
- FeCl₂ and FeCl₃ mitigated *mmoX* and *pmoA* downward, and FeCl₃ decreased *mcrA*.
- FeCl₂ and FeCl₃ increased NH₄⁺-N content, *nirK* and *norB*, and FeCl₃ declined *nosZ*.

GRAPHICAL ABSTRACT



ARTICLE INFO

Keywords:
Composting
Swine manure
Fe salts
Fe minerals
Greenhouse gases
Ammonia

ABSTRACT

Greenhouse gases (GHGs) and ammonia (NH₃) emissions from livestock and poultry manure composting are a crucial environmental problem worldwide. In this study, effects of ten soluble iron (Fe) salts or insoluble Fe and Fe minerals on carbon dioxide (CO₂), methane (CH₄), nitrous oxide (N₂O) and NH₃ emissions were systematically explored in swine manure composting, respectively. Results illustrated that soluble Fe salts were superior to insoluble Fe minerals on reducing global warming potential (GWP) of GHGs. Furthermore, Fe(III) salts were more effective on weakening CH₄, NH₃ and CO₂ emissions compared to Fe(II) salts. Specifically, 35.7 % and 67.3 % of CH₄ reduction was attributed that ferrous chloride (FeCl₂) and ferric chloride (FeCl₃) increased initial oxidation reduction potential (ORP) and mitigated *mmoX* and *pmoA* downward in initial composting. Abundances of *mmoX* and *pmoA* decreased by 45.9 % and 76.3 % in Ctrl treatment, 37.9 % and 60.7 % in FeII treatment, 25.7 % and 51.9 % in FeIII treatment, respectively. In addition, main methanogenic archaea of *Methanobrevibacter* abundances in Ctrl, FeII and FeIII obviously decreased by 82.2 %, 89.3 % and 92.2 % in the first 10 days, respectively.

* Corresponding author. National Engineering Research Center for Safe Sludge Disposal and Resource Recovery, Harbin Institute of Technology, Harbin, 150090, China.

** Corresponding author.

E-mail addresses: hitwk@sina.com (K. Wang), zhengruilun@baafs.net.cn (R. Zheng).

Moreover, Fe(III) salts enhanced N₂O emission relative to Ctrl and Fe(II) salts. NH₄⁺-N content, *nirK* and *norB* increment might promote N₂O release in initial period. Notedly, *nosZ* of Ctrl and FeII separately ascended by 71.2 % and 66.9 %, yet *nosZ* of FeIII descended by 45.8 % in the first 10 days, which might restrict denitrification. Generally, this study proposed a valuable and feasible strategy to alleviate GHGs emissions and nitrogen loss in composting.

1. Introduction

Massive swine manure is inevitably produced from swine industry, which contains abundant nutrients essential for plant growth (Parodi et al., 2021; Shen et al., 2015). Hence, how to properly and effectively treat swine manure is critical. Composting is one of conventional biological techniques, in which microbes decompose organic wastes such as manure into stabilized humus with high agronomic value (Fan et al., 2021a, 2021b; Wang et al., 2024a). Unfortunately, numerous greenhouse gases (GHGs) including carbon dioxide (CO₂), methane (CH₄), nitrous oxide (N₂O) and malodorous gas containing ammonia (NH₃) are emitted from composting due to different biochemical reactions, which cause fertilizer efficiency decrement and a series of serious environmental problems, especially greenhouse effect and air pollution (Guo et al., 2020b; Xu et al., 2024).

Massive CO₂ is produced from aerobic composting because of microbial respiration (Cao et al., 2023), which could indirectly reflect reaction extent of composting (Wang et al., 2022b). Zhang et al. (2021) reported that nitrogen loss took up roughly 30 % in swine manure composting. Meanwhile, NH₃ release is the largest single share of nitrogen loss, accounting for approximately 80 % (Shan et al., 2021). Additionally, N₂O is the byproduct from denitrification in composting matrix, closely associating with functional genes to encode corresponding enzymes (containing nitrate, nitrite, nitric oxide and nitrous oxide reductase) (Dai et al., 2022; Wang et al., 2018; Zhou et al., 2022). Similarly, CH₄ emission goes in hand with enzymes (methanogenesis, methane monooxygenase and dehydrogenase) encoded by functional genes (He et al., 2019; Wen et al., 2021; Zhang et al., 2024). Moreover, CH₄ and N₂O are generated by microorganisms involved in anaerobic environment of composting (Ge et al., 2018; Shen et al., 2011).

As a whole, in addition to microbes and functional genes, it was summarized that massive factors may affect GHGs and NH₃ emissions from composting, principally comprising of feedstocks types, process parameters, environmental factors (mainly including aeration, temperature, pH, moisture content, C/N ratio), and so on (Jiang et al., 2011; Liu et al., 2023; Shan et al., 2021). Compared to the complexity and cost of changing composting feedstocks or process parameters, using diverse conditioners to regulate GHGs and NH₃ emissions by adjusting environmental factors is an economical and viable means. Conditioners generally consist of chemical, physical and biological types. Notably, selection of appropriate biological conditioner highly relies on composting feedstocks and environmental factors, thereby hindering its practical application. Furthermore, most physical conditioners such as biochar weakened GHGs and NH₃ emissions by adjusting oxygen environment inside composting and adsorption (He et al., 2017; Wang et al., 2024b). However, adsorption capacity may be restricted by saturated adsorption sites. Consequently, Cao et al. (2019) reported that chemical conditioners were more suitable than biological and physical conditioners on declining abovementioned gases.

Recently, chemical conditioners have attracted growing attentions, and presented diverse impacts on GHGs and NH₃ emissions from composting (Zhang et al., 2021). Combinations of magnesium and phosphorus-related conditioners were widely used into composting, aiming to alleviate nitrogen loss via the formation of stable Mg(NH₄)PO₄·6H₂O (Hoang et al., 2022). Moreover, Jiang et al. (2016) documented that MgO and H₃PO₄, MgSO₄ and KH₂PO₄, MgSO₄ and Ca(H₂PO₄)₂, MgSO₄ and H₃PO₄ showed different potentials on GHGs and NH₃ emissions from swine manure composting. Importantly, excessive

magnesium and phosphorus-related conditioners could inhibit organic matters (OMs) biodegradation in composting. Furthermore, MgO increased pH of composting, which may be harmful to microbial activity and prolonged the composting period (Jiang et al., 2016). Notedly, individual magnesium or phosphorus-related conditioners were difficult to realize drastic GHGs and NH₃ emissions reduction. Additionally, high price of phosphorus conditioners might restrict its practical applications.

As mentioned above, GHGs and NH₃ emissions from composting highly depended on types of feedstocks and conditioners. In this study, as preliminary experiments, five soluble Fe salts (FeCl₂; FeCl₃; FeSO₄; Fe₂(SO₄)₃; Fe(NO₃)₃) and five insoluble Fe or Fe minerals (zero-valent iron, ZVI; goethite; hematite; magnetite; pyrite) were aerobic assisted-composted with swine manure, respectively, in order to investigate influences on GHGs and NH₃ emissions from composting. As shown in Table 1, soluble Fe salts were superior to insoluble Fe and Fe minerals on reducing global warming potential (GWP) of GHGs. Based on preliminary experiments results (more details seen in Supporting information), FeCl₂ and FeCl₃ representing typical Fe(II) and Fe(III) salts were selected to separately aerobic assisted-compost with swine manure, aiming to further explore and compare impacts on: i) alterations of indicative physicochemical properties, different forms of nitrogen (total dissolved nitrogen, TDN; NH₄⁺-N; NO₃⁻-N; NO₂⁻-N) and Fe (soluble Fe²⁺, SFe²⁺; soluble Fe³⁺, SFe³⁺; insoluble Fe, ISFe) contents; ii) changes of typical microbes, nitrogen and methane-related metabolism genes abundances. So as to elucidate underlying mechanisms on GHGs and NH₃ emissions, meanwhile, proposing a feasible and economical way to alleviate greenhouse effect caused by composting.

2. Material and methods

2.1. Composting materials and process

Feedstock used in composting was fresh swine manure, which was gathered from a livestock farm in Harbin, northeast China. Rice husk collected from local farm in Harbin was utilized as the bulking agent. Afterwards, rice husk was thoroughly blended with swine manure at the weight ratio of 1:4. Characteristics of two feedstocks were displayed in Table S1 (Supporting information). Three treatments containing composting of swine manure alone, and assisted-composting of swine manure with 3 % FeCl₂ and 3 % FeCl₃ (based on swine manure dry weight) were carried out, which named as Ctrl, FeII and FeIII for short, respectively. Notedly, FeCl₂ and FeCl₃ were introduced to composting feedstocks in the form of solution.

Mixed materials were loaded into three cylindrical plexiglass reactors (40 L of volume, 0.4 m of diameter × 1.0 m of height) lasting for 60 days to obtain final products. In order to avoid excessive heat loss, three reactors were placed in a hot water bath and the temperature of it was mediated nearly to that of composting system ($\pm 2^{\circ}\text{C}$). Temperature was recorded three times per day by thermometers and separately calculated their means. Fresh air was continuously supplied at 1 L/min from the bottom into reactors for aerobic composting condition, and gases were discharged by a pipe at the bottom of reactors. During composting, NH₃ was absorbed by boric acid, CH₄, CO₂ and N₂O were gathered by gas collect bags. Composting samples were collected from nine different locations in three depths of reactors, subsequently mixed homogenously to one representative sample for further analysis.

2.2. Analysis of physicochemical properties

Moisture content of sample was detected by weight loss, which was dried at 105 °C to the constant weight. After that, volatile solid (VS) content of dried sample was measured by weight loss at 550 °C in a muffle furnace for 4 h. Samples were extracted by deionized water when solid-liquid ratio at 1:10, then shook at 180 rpm in an incubator shaker for 2 h and centrifuged at 4000 rpm, pH and oxidation reduction potential (ORP) of supernatant were measured by a pH/ORP meter (PHSJ4F, China). After centrifuging at 12000 rpm, supernatant was filtered through the 0.45 µm membrane for the determination of dissolved organic carbon (DOC) and TDN. A total organic carbon analyzer (TOC-V_{CPH}, SHIMADZU) was applied to detect DOC and TDN concentrations. Fresh sample was extracted by Al₂(SO₄)₃ solution (0.1 mol/L, pH of 2.0), and obtained SFe²⁺ and SFe³⁺ in supernatant via shaking and centrifuging. Additionally, ISFe in sample was digested by perchloric acid-nitric acid. Thereafter, SFe²⁺, SFe³⁺ and ISFe contents were immediately determined using 1,10-o-phenanthroline method by a UV-visible spectrophotometer. According to Wang et al. (2018), 2 mol/L KCl solution was utilized to extract NH₄⁺-N, NO₃⁻-N and NO₂⁻-N in sample at solid-liquid ratio of 1:10. NH₄⁺-N content was analyzed by an ultraviolet and visible spectrophotometer (UN754, China), NO₃⁻-N and NO₂⁻-N contents were detected by an ion chromatograph (ICS-3000, DIONEX). Considering emissions rate of gases, NH₃ was detected by acid-base titration with sulfuric acid, CH₄, CO₂ and N₂O were monitored by a gas chromatograph (7890A, Agilent) (Wang et al., 2022a).

2.3. DNA extraction and functional genes quantification

0.5 g composting samples were applied to extract DNA by the MagBind® Soil DNA Kit (Omega Bio-tek, USA) according to manufacturer's requirements, and each sample was extracted in triplicate. Microbial community was tested by 16S rRNA high-throughput sequencing. DNA extraction was quantified by the NanoDrop 2000 spectrophotometer (Thermo Fisher Scientific, USA) and then kept at -80 °C for further analysis. Abundances of nitrogen and methane-related metabolism genes were determined by quantitative polymerase chain reaction (qPCR). In detail, primer sequences for functional genes, 16S rRNA gene sequencing and corresponding quantitative methods referred to Wang et al. (2022a).

2.4. Data and statistical analysis

All analyses were performed in triplicate, and data were displayed as mean ± standard deviation. Means and standard deviations were analyzed by Excel (2019) (Microsoft Office, 2019; Microsoft, USA). One-way analysis of variance (ANOVA) and least significant difference (LSD)

test at level of $p < 0.05$ were applied to estimate significant difference. Statistical analysis was conducted by SPSS 22.0 (IBM, USA), graphs were drawn by R 3.2.2 (R Core Team, 2018) and Origin 2021 (Origin Lab, USA).

3. Results and discussion

3.1. Changes of physicochemical properties

Temperature and pH as governing indicators are strongly correlated with the biodegradation of OMs by affecting microorganisms activity (Ma et al., 2022; Wang et al., 2021). In this study, the entire composting period was divided into heating (from Day 0 to Day 1), thermophilic (from Day 1 to Day 12), cooling (from Day 12 to Day 32) and mature period (from Day 32 to Day 60) by the alteration of temperature (Fig. 1a). Temperature of Ctrl, FeII and FeIII sharply rose into thermophilic period (≥ 50 °C) within 1 day, and reached the highest of 64.0, 61.4 and 61.3 °C on Day 3, respectively, then kept above 50 °C until Day 12. High temperature was helpful to the inactivation of pathogens in composting (Chen et al., 2022). Ultimately, with the depletion of bioavailable OMs, temperature of three reactors progressively decreased to room temperature.

FeCl₂ and FeCl₃ as acidic salts separately reduced initial pH by 5.6 % and 9.3 % (Fig. 1b). In 60 days composting, pH of Ctrl, FeII and FeIII rose from 7.2, 6.8 and 6.6 to the highest of 8.9, 8.7 and 8.7 in the first 5 days, then steadily fell to 8.0, 7.5 and 7.4 at the end of composting, respectively. The augmentation of pH was ascribed to the accumulation of NH₄⁺-N (Fig. 2d) via mineralizing organic nitrogen in feedstocks (Chen et al., 2020; Xue et al., 2021). Subsequently, organic acidic release and NH₃ volatilization in thermophilic period promoted the stable decrement of pH. Notedly, FeCl₂ and FeCl₃ were conducive to NH₄⁺-N reservation by decreasing pH, moreover, NH₄⁺-N content of FeIII was higher than that of FeII. Jiang et al. (2011) reported that high NH₄⁺-N content may inhibit microbial activity. Consequently, temperature of FeII and FeIII was lower than that of Ctrl on the same day, possibly attributed to the limitation of microbial activity. Furthermore, Fe²⁺ and Fe³⁺ hydrolysis may promote the formation of pore structure inside composting materials, therefore improving air permeability and more heat was lost with the evaporation of water. Moisture contents of Ctrl, FeII and FeIII steadily diminished to 50.3 %, 48.3 % and 47.4 % on Day 60 respectively (Fig. 1c). There was no doubt that the most apparent descent occurred in thermophilic period.

Since ORP was a decisive factor probably associating with CH₄ emission (Wang et al., 2015, 2022a), it was essential to explore the change of ORP during composting. As depicted in Fig. 1d, it was worth noting that FeCl₂ and FeCl₃ enhanced initial ORP by 26.3 % and 134.8 %, respectively. Moreover, ORP of Ctrl, FeII and FeIII all dramatically

Table 1

Cumulative emissions of greenhouse gases (GHGs) and NH₃, and GHGs global warming potential (GWP) of Ctrl20, FeCl₃, FeCl₂, Fe₂(SO₄)₃, FeSO₄, Fe(NO₃)₃, zero-valent iron, goethite, hematite, magnetite, and pyrite relative to CO₂ in 20 days composting. Ctrl20, FeCl₃, FeCl₂, Fe₂(SO₄)₃, FeSO₄, Fe(NO₃)₃, zero-valent iron, goethite, hematite, magnetite, and pyrite denoted composting of swine manure alone, and assisted-composting of swine manure with 3 % FeCl₃, FeCl₂, Fe₂(SO₄)₃, FeSO₄, Fe(NO₃)₃, zero-valent iron, goethite, hematite, magnetite and pyrite, respectively.

Treatment	Cumulative emissions (mg/g)				GWP of CO ₂ equivalents (mg/g)				
	NH ₃	CO ₂	CH ₄	N ₂ O	CO ₂	CH ₄	N ₂ O	CO ₂ + CH ₄ + N ₂ O	CH ₄ + N ₂ O
Ctrl20	10.41	641.66	0.82	0.0075	641.66	61.34	2.05	705.05	63.39
FeCl ₃	7.58	464.10	0.43	0.0100	464.10	32.16	2.73	498.99	34.89
FeCl ₂	7.96	525.47	0.49	0.0092	525.47	36.65	2.51	564.63	39.16
Fe ₂ (SO ₄) ₃	9.23	590.00	0.47	0.0087	590.00	35.16	2.38	627.54	37.54
FeSO ₄	9.66	610.35	0.63	0.0084	610.35	47.12	2.29	659.95	49.60
Fe(NO ₃) ₃	11.99	656.97	0.14	1.1874	656.97	10.47	324.16	991.60	334.63
Zero-valent iron	10.56	667.57	0.78	0.0110	667.57	58.34	3.00	728.91	61.34
Goethite	9.05	629.44	0.58	0.0097	629.44	43.38	2.65	675.47	46.03
Hematite	9.86	634.24	0.51	0.0115	634.24	38.15	3.14	675.53	41.29
Magnetite	10.15	621.35	0.56	0.0085	621.35	41.89	2.32	665.56	44.21
Pyrite	8.74	675.25	0.49	0.0101	675.25	36.65	2.76	714.66	39.41

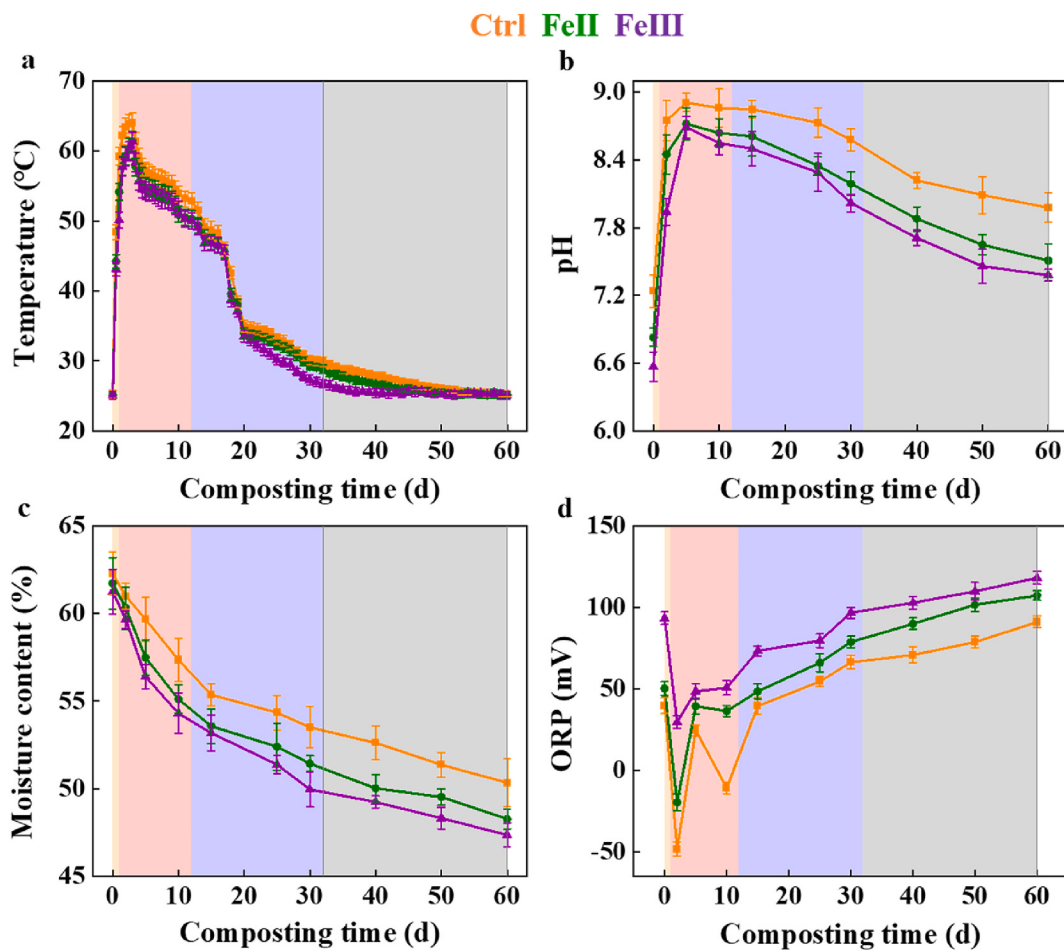


Fig. 1. Changes of temperature (a), pH (b), moisture content (c) and oxidation reduction potential (ORP) (d) in Ctrl, FeII and FeIII during 60 days swine manure composting, respectively. Ctrl, FeII and FeIII denoted composting of swine manure alone, and assisted-composting of swine manure with 3 % FeCl_2 and 3 % FeCl_3 , respectively. Different background colors represented four periods of composting. From left to right was heating period (light yellow), thermophilic period (light red), cooling period (light blue) and mature period (light grey), respectively. (For interpretation of the references to color in this figure legend, the reader is referred to the Web version of this article.)

declined from 39.7, 50.2 and 93.3 mV to -48.3 , -19.4 and 29.5 mV in the first 2 days, respectively. Pearson correlation analysis (Fig. 4) demonstrated that ORP presented the negative correlation with CH_4 emission, indicating that relatively low ORP provided a satisfactory environment for CH_4 production (Fig. 3b). Subsequently, ORP of three treatments gradually ascended in cooling and mature period via various biochemical oxidation reactions, because of the more oxygen diffusion and lower moisture content than those in early phase.

3.2. VS, DOC, TDN, NH_4^+ -N, NO_3^- -N and NO_2^- -N

Fig. 2a demonstrated that VS contents of Ctrl, FeII and FeIII significantly descended by 38.0 %, 35.3 % and 34.2 % ($p < 0.05$) in 60 days composting, respectively, which was possibly attributed to the mineralization of OMs and loss in forms of CO_2 and CH_4 (Qu et al., 2020). As depicted in Fig. 2b, variation trend of DOC contents mirrored that of VS contents in three treatments. Notedly, both VS and DOC contents greatly reduced within thermophilic period, reflecting that thermophilic period was the dominant stage for OMs biodegradation, accordingly, CO_2 emission concentrated in this period (Fig. 3d). Moreover, VS and DOC contents reduction in mature period were both unapparent, suggesting that composting materials were stable. As abovementioned, FeCl_2 and FeCl_3 both hindered the use of OMs by microbes. Consequently, VS and DOC contents of FeII and FeIII were both apparently higher than those of Ctrl. Similarly to previous study (Xie et al., 2023), Fig. 4 confirmed that

carbon (VS and DOC) contents were highly positive correlations with different forms of nitrogen (TDN, NH_4^+ -N, NO_3^- -N and NO_2^- -N) contents in this research.

When discussing NH_3 and N_2O emissions from composting, it is necessary to investigate alterations of different nitrogen forms contents. In heating period, TDN contents of three treatments all elevated because of the biodegradation of N-containing compounds (Fig. 2c). Additionally, NH_4^+ -N contents of three treatments all significantly ascended in the first 5 days and then steadily descended by the end (Fig. 2d). Specifically, notable augmentation of NH_4^+ -N content was observed in Ctrl, FeII and FeIII by 168.5 %, 180.8 % and 190.9 % ($p < 0.05$) over the first 5 days, respectively, due to ammonification. FeCl_2 and FeCl_3 improved the acidity of composting, thereby hindering NH_3 emission and remaining more NH_4^+ -N. Subsequently, NH_4^+ -N contents of Ctrl, FeII and FeIII sharply decreased by 88.6 %, 75.3 % and 70.3 % ($p < 0.05$) from Day 5 to Day 60, respectively, meaning that NH_3 emission of Ctrl was the maximum among three runs. In thermophilic period, the utilization of nitrogen-containing substances by microorganisms and NH_3 volatilization likely led to the noticeable decrement of TDN and NH_4^+ -N contents (Huang et al., 2022).

Fig. 2e, f displayed that NO_3^- -N and NO_2^- -N contents were extremely lower than NH_4^+ -N content in composting materials. Concerning NO_3^- -N content, Ctrl, FeII and FeIII generally presented a decreasing trend throughout 60 days composting, and ultimately declined to 0.27, 0.22 and 0.14 mg/g, respectively. Particularly, there was a remarkable

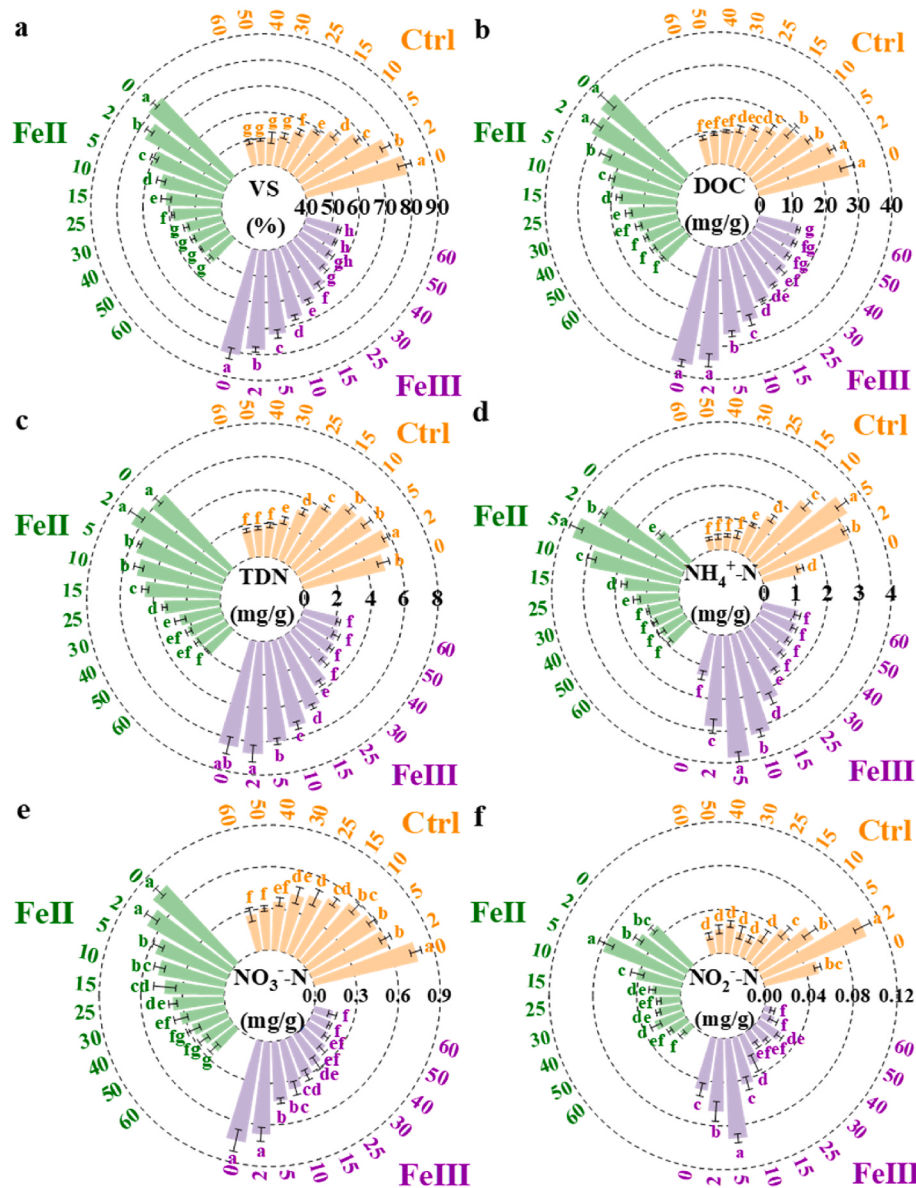


Fig. 2. Contents of volatile solid (VS) (a), dissolved organic carbon (DOC) (b), total dissolved nitrogen (TDN) (c), NH_4^+ -N (d), NO_3^- -N (e) and NO_2^- -N (f) in Ctrl, FeII and FeIII during 60 days swine manure composting, respectively. Ctrl, FeII and FeIII denoted composting of swine manure alone, and assisted-composting of swine manure with 3 % FeCl_2 and 3 % FeCl_3 , respectively. Different letters above columns represented significant differences at $p < 0.05$ among composting days in the identical treatment.

downward of 22.1 % ($p < 0.05$) in Ctrl over the first 2 days, corresponding to the notable onward of NO_2^- -N content by 102.0 % ($p < 0.05$) in the same time, seeming that denitrification principally occurred in initial composting of Ctrl, and resulted in N_2O generation (Fig. 3c). However, NO_3^- -N contents in FeII and FeIII obviously dropped by 27.6 % and 41.9 % ($p < 0.05$) in the first 5 days, corresponding to the distinct ascent of NO_2^- -N content by 59.2 % and 87.8 % ($p < 0.05$) from Day 0 to Day 5, seeming that FeCl_2 and FeCl_3 delayed denitrification and N_2O generation in composting (Fig. 3c). Finally, NO_2^- -N contents in three trials fluctuated and fell to the range of 0.008–0.017 mg/g on Day 60.

3.3. Emissions of GHGs and NH_3

As shown in Fig. 3a, in accordance with prior studies (Li et al., 2024; Shan et al., 2021), NH_3 emission concentrated in thermophilic period, because of abundant NH_4^+ -N integrated with hydroxyl ion, high temperature and water evaporation (Ren et al., 2021). Furthermore, peak

NH_3 release rates of Ctrl, FeII and FeIII were 3.23, 2.73 and 2.53 mg $\text{d}^{-1}\cdot\text{g}^{-1}$, respectively. On account of temperature and pH decrement, consumption of NH_4^+ -N, NH_3 emission rate levelled off to zero and cumulative emission tended to be stable in cooling period. Importantly, FeCl_2 and FeCl_3 obviously reduced peak emission rate and cumulative emission of NH_3 . It was observed in Pearson correlation analysis (Fig. 4) that NH_3 emission rate was positively relevant with NH_4^+ -N content, temperature and pH of composting materials, in accordance with Chen et al. (2020). Specifically, FeCl_2 and FeCl_3 dramatically declined cumulative NH_3 emissions by 30.8 % and 37.3 % ($p < 0.05$), respectively. Overall, combining swine manure with FeCl_3 or FeCl_2 assisted-composting is viable to mitigate the concern of nitrogen loss.

The consumption of oxygen by microorganisms and high moisture content in inner area of feedstocks produced anaerobic environment in initial composting, which was conducive to CH_4 discharge. There were two remarkable peaks of CH_4 emission rate in three trials (Fig. 3b). The first peak was 153.06 mg $\text{d}^{-1}\cdot\text{kg}^{-1}$ of Ctrl, 249.47 mg $\text{d}^{-1}\cdot\text{kg}^{-1}$ of FeII

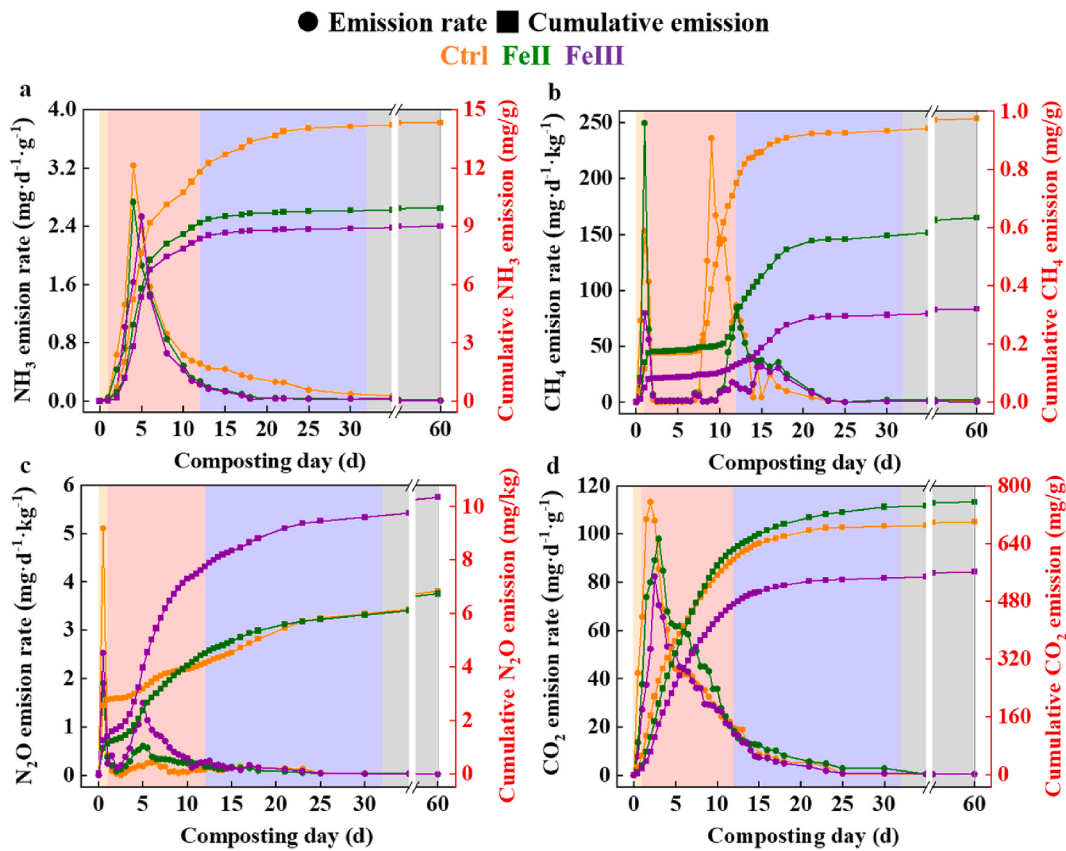


Fig. 3. Emission rates and cumulative emissions of NH₃ (a), CH₄ (b), N₂O (c) and CO₂ (d) in Ctrl, FeII and FeIII during 60 days swine manure composting, respectively. Ctrl, FeII and FeIII denoted composting of swine manure alone, and assisted-composting of swine manure with 3 % FeCl₂ and 3 % FeCl₃, respectively. Different background colors represented four periods of composting. From left to right was heating period (light yellow), thermophilic period (light red), cooling period (light blue) and mature period (light grey), respectively.

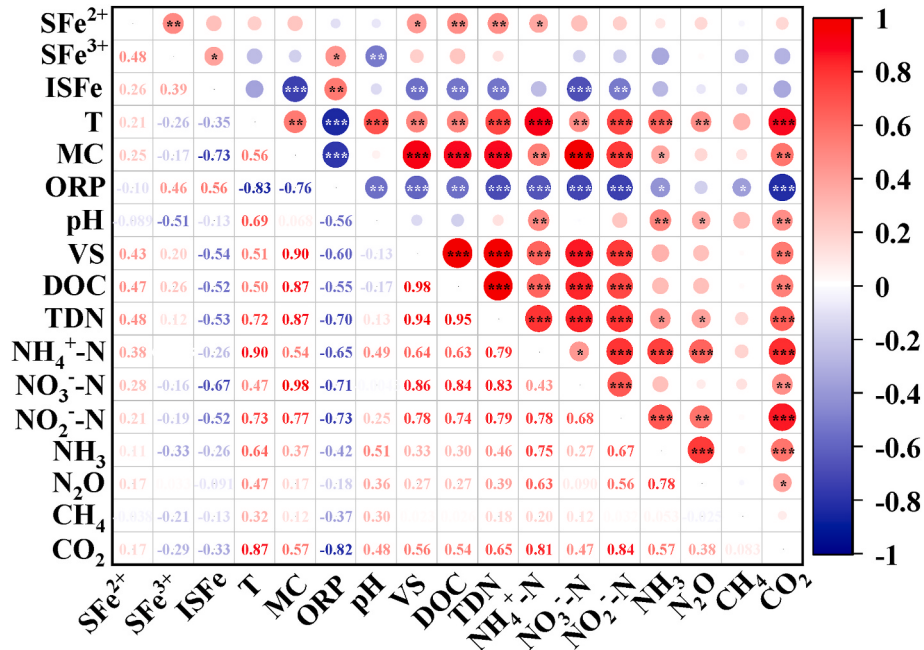


Fig. 4. Pearson correlation analysis between environmental factors (contents of soluble Fe²⁺, SFe²⁺; soluble Fe³⁺, SFe³⁺; insoluble Fe, ISFe; temperature, T; moisture content, MC; oxidation reduction potential, ORP; pH; contents of volatile solid, VS; dissolved organic carbon, DOC; total dissolved nitrogen, TDN; NH₄⁺-N; NO₃⁻-N; NO₂⁻-N) and gases (NH₃; N₂O; CH₄; CO₂) emission rate in 60 days swine manure composting. Red and blue discs represented positive and negative relationships, respectively. The diameter and color depth of the disc were proportional to the magnitude of correlation coefficient. Levels of significance: * $p < 0.05$, ** $p < 0.01$, *** $p < 0.001$.

and 79.68 mg d⁻¹.kg⁻¹ of FeIII, respectively, and all emerged on Day 1. FeCl₃ obviously enhanced ORP (Fig. 1d), therefore limiting CH₄ emission in initial composting. On the contrary, Fe²⁺ of FeCl₂ might be an electron donor and promote microbial methanogenesis (Yin et al., 2018; Zhang et al., 2024). Notedly, CH₄ discharge almost vanished in thermophilic period of all tests because of high temperature and the rapid ORP increment. With the gradual decline of temperature, CH₄ discharge rate rose again and reached the second peak of 236.06 (of Ctrl), 84.58 (of FeII) and 32.41 mg d⁻¹.kg⁻¹ (of FeIII), respectively. Ultimately, CH₄ emissions of all trials nearly disappeared in mature period. Generally, FeCl₂ and FeCl₃ both distinctly descended cumulative CH₄ emission by 35.7 % and 67.3 % ($p < 0.05$), which proposed an effective strategy to realize CH₄ emission reduction.

As displayed in Fig. 3c, N₂O emission rates of Ctrl, FeII and FeIII all dramatically ascended and separately reached the maximum of 5.11, 1.90 and 2.53 mg d⁻¹.kg⁻¹ in heating period, probably ascribed to denitrification of NO₃⁻-N (Guo et al., 2020a). Afterwards, N₂O production sharply diminished in thermophilic period. The phenomenon was possibly attributed to rapid degradation of OMs, further improving aeration porosity and O₂ content of composting, thereby restraining propagation of anaerobic microorganisms (Du et al., 2024). Importantly, besides NO₂⁻-N content, NH₄⁺-N content also presented a positive relationship with N₂O emission rate (Fig. 4), implying that abundant NH₄⁺-N as substrate was provided for nitrification/denitrification to N₂O production. In summary, the most cumulative N₂O emission was observed in FeIII of 10.34 mg/kg, followed by Ctrl of 6.83 mg/kg, and lastly FeII of 6.74 mg/kg.

Analogously to NH₃, CO₂ release primarily emerged in thermophilic period (Fig. 3d). CO₂ emission rates of Ctrl, FeII and FeIII swiftly rose in heating period due to rapid utilization of readily degradable carbon, and separately achieved the peak of 113.31, 98.03 and 82.44 mg d⁻¹.g⁻¹ in thermophilic period, because high temperature stimulated mineralization of OMs. There was no doubt that besides temperature, VS, DOC and different forms of nitrogen contents showed positive relationships with CO₂ emission rate (Fig. 4). Afterwards, with the removal of biodegradable OMs, CO₂ emission rate steadily fell, and eventually disappeared in mature period of all tests. Notedly, FeCl₃ obviously weakened cumulative CO₂ emission by 19.7 % ($p < 0.05$), however, FeCl₂ had no significant impact on cumulative CO₂ emission.

3.4. Changes of microbial community

Microbes are crucial indicators, which might affect GHGs emissions from composting (Guo et al., 2020a, 2020b). Composting materials in three treatments of four typical days (Day 0 of initial composting, Day 10 of thermophilic period, Day 30 of cooling period and Day 60 of mature period) were selected to investigate microbial community structures succession (Fig. S3, Supporting information). Importantly, CH₄ release goes in hand with metabolism of archaea (Du et al., 2024), therefore methanogenic archaea of genus relative abundances in composting matrix were further analyzed (Fig. S4, Supporting information). *Methanobrevibacter* was the main genus of methanogenic archaea in each test, which stimulated the transformation of CO₂ into CH₄ (Samuel et al., 2007). As composting progressed, *Methanobrevibacter* abundances in Ctrl, FeII and FeIII obviously decreased by 82.2 %, 89.3 % and 92.2 % in the first 10 days, respectively, suggesting that CH₄ production from composting principally occurred in initial stage. Moreover, FeCl₂ and FeCl₃ both showed suppressive effects on *Methanobrevibacter* activity, and the effect of FeCl₃ was more drastic.

3.5. Genes related to nitrogen metabolism

In order to have a comprehensive understanding on effects of FeCl₂ and FeCl₃ on NH₃ and N₂O emissions, we further chose four representative days (identical to the day selection of microbial community) to explore alterations of typical nitrogen metabolism-related genes.

Changes of ammonification-involved genes relative abundances were presented in Fig. S5 (Supporting information). Importantly, abundances of nitrification/denitrification-associated functional genes (*amoA*, *nxrA*, *narG*, *nirK*, *norB* and *nosZ*) were characterized by qPCR, and shown in Fig. 5. Gene of *amoA* is responsible for converting NH₄⁺-N into NH₂OH (Jiang et al., 2021; Li et al., 2024). The extremely low abundances of *amoA* in three treatments on Day 0 implied that scarce NH₄⁺-N was oxidized in initial composting. Subsequently, *amoA* in Ctrl, FeII and FeIII all obviously enhanced from around 1.02×10^7 copies/g on Day 0– 1.73×10^7 , 8.06×10^7 and 2.52×10^7 copies/g on Day 10, and further increased to 5.41×10^7 , 2.38×10^8 and 1.54×10^8 copies/g on Day 30 (Fig. 5a), respectively, demonstrating that FeCl₂ and FeCl₃ promoted the oxidation of NH₄⁺-N to NH₂OH during composting. Additionally, drastic *amoA* ascent of FeII in early composting was conducive to weaken the inhibitory effect of high NH₄⁺-N concentration on microbial activity. After that, NH₂OH was oxidized to NO₂⁻-N, and further to NO₃⁻-N by *nxrA*. Contrary to variation tendency of *amoA*, *nxrA* abundances dramatically declined from 5.10×10^5 to 2.92×10^4 copies/g of Ctrl, from 4.91×10^5 to 2.50×10^4 copies/g of FeII, and from 4.80×10^5 to 2.13×10^4 copies/g of FeIII in the entire composting (Fig. 5b).

NO₃⁻-N reductase (*narG*) and NO₂⁻-N reductase (*nirK*) genes are critical roles in denitrification, which separately bind to the reduction of NO₃⁻-N to NO₂⁻-N (first step) and NO₂⁻-N to NO (rate-limiting step) (Liu et al., 2020, 2024; Qin et al., 2021). Afterwards, NO reductase (*norB*) gene facilitates the conversion of NO into N₂O, as a result, *norB* abundance closely correlates with N₂O emission. Ultimately, N₂O is transformed to N₂ by N₂O reductase (*nosZ*) gene (Xie et al., 2023; Xu et al., 2024). As displayed in Fig. 5c, *narG* in Ctrl, FeII and FeIII were 3.98×10^6 , 2.34×10^6 and 3.33×10^6 copies/g on Day 0, respectively, illustrating that more NO₃⁻-N was converted into NO₂⁻-N in Ctrl, thereby providing sufficient substrates for N₂O production during initial composting. Subsequently, *narG* in Ctrl, FeII and FeIII sharply descended by 85.5 %, 56.5 % and 84.0 % ($p < 0.05$) from Day 0 to Day 10. Importantly, *nirK* in Ctrl, FeII and FeIII on Day 0 were extremely low (Fig. 5d), then distinctly ascended to 6.04×10^7 , 1.72×10^8 and 2.24×10^8 copies/g on Day 10, respectively, revealing that FeCl₃ versus FeCl₂ further facilitated the reduction of NO₂⁻-N into NO.

As shown in Fig. 5e, *norB* in Ctrl, FeII and FeIII swiftly ascended and reached the maximum of 9.07×10^7 , 1.33×10^8 and 1.67×10^8 copies/g on Day 10, then steadily fell to 5.83×10^7 , 7.53×10^7 and 9.66×10^8 copies/g on Day 60, respectively. Notedly, *norB* in FeIII was apparently higher than those in the other two tests on the same day (except Day 0), seeming that *norB* gene increment may be the decisive factor leading to more N₂O emission of FeIII. Although FeCl₂ evidently enhanced *nirK* and *norB* abundances in thermophilic and cooling period, FeCl₂ had no obvious influence on N₂O release, since abundance of *nosZ* in FeII was significantly higher than those in Ctrl and FeIII (Fig. 5f), and promoted transformation of N₂O into N₂. Importantly, *nosZ* in FeIII maintained the least level among three treatments throughout the entire composting except Day 0, meaning that FeCl₃ restricted *nosZ* expression, and resulted in the least N₂O converted to N₂. In detail, *nosZ* in Ctrl and FeII steadily increased from 9.66×10^6 and 1.84×10^7 copies/g on Day 0– 5.06×10^7 and 8.44×10^7 copies/g on Day 60, respectively, while *nosZ* in FeIII firstly decreased from 1.70×10^7 copies/g on Day 0 to the least of 9.20×10^6 copies/g on Day 10, then gradually increased to 3.00×10^7 copies/g on Day 60. Generally, in addition to the apparent elevation of NH₄⁺-N content providing substrate for nitrification/denitrification, FeCl₃ improving N₂O emission was probably attributed to the ascent of both *nirK* and *norB*, and the descent of *nosZ*.

We further explored relationships between six nitrification/denitrification-associated genes and environmental factors (containing physicochemical properties, different forms of nitrogen and iron contents) by principal component analysis (PCA) in Fig. 7a, and random forest analysis (RFA) was conducted to study contributions of environmental factors and genes to N₂O discharge (Fig. 7b). Xie et al. (2023) reported that organic carbon and nitrogen indirectly impacted genes

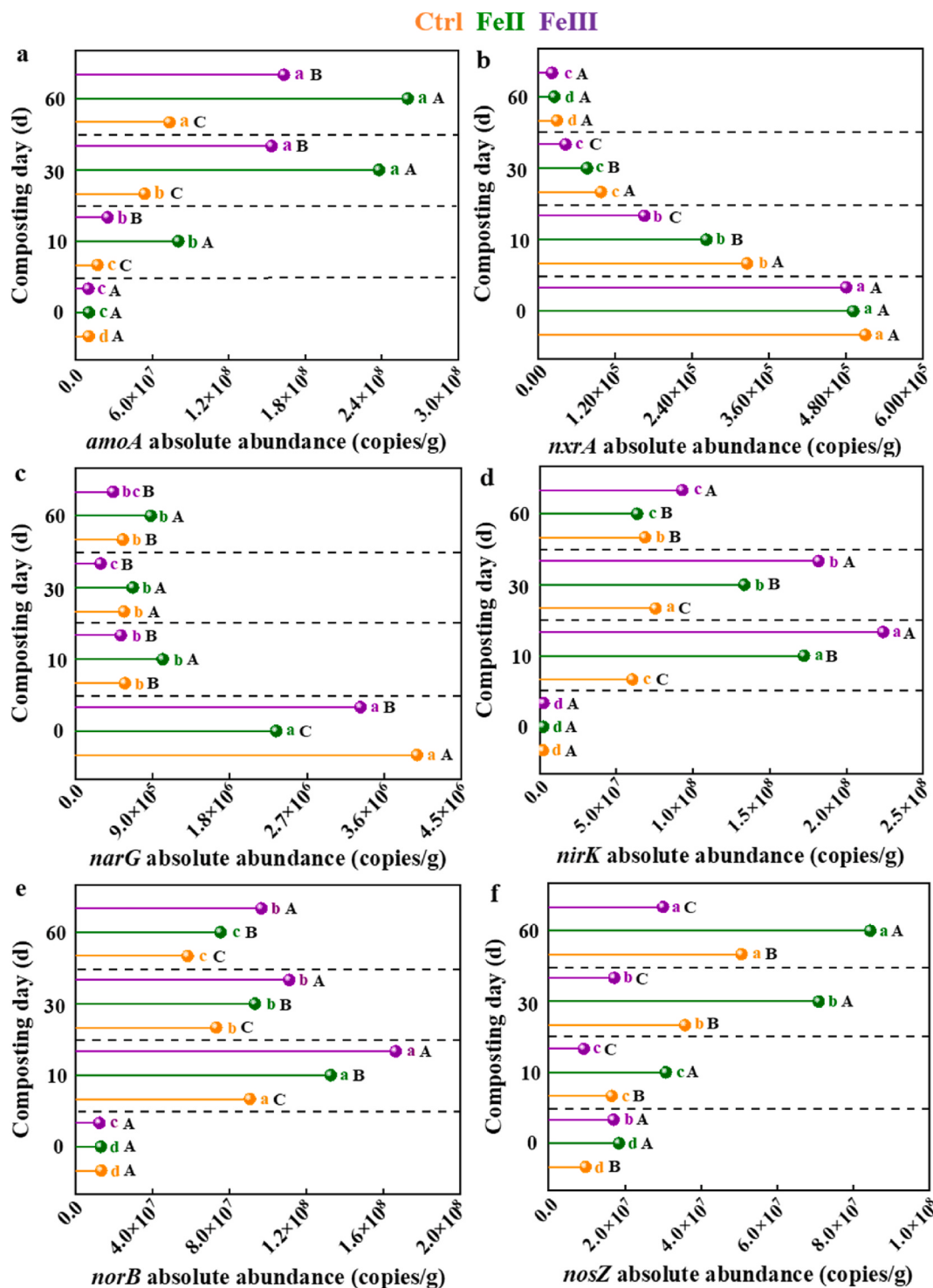


Fig. 5. Abundances of nitrification/denitrification-associated genes (*amoA*, a; *nxrA*, b; *narG*, c; *nirK*, d; *norB*, e; *nosZ*, f) in Ctrl, FeII and FeIII on Day 0, 10, 30 and 60 of 60 days swine manure composting, respectively. Ctrl, FeII and FeIII denoted composting of swine manure alone, and assisted-composting of swine manure with 3 % FeCl₂ and 3 % FeCl₃, respectively. Capital letters above spheres denoted significant differences at $p < 0.05$ among three treatments on the identical day. Lowercase letters in the same color above spheres represented significant differences at $p < 0.05$ among composting days in the same treatment.

abundances via regulating corresponding microbes. Consequently, different forms of nitrogen contents variations strongly impacted on genes involved in nitrification/denitrification. Similarly to *nosZ*, abundance of *amoA* was positively correlated with ISFe content (Table S2, Supporting information), and negatively correlated with moisture content and ORP, contents of VS, DOC, TDN and NH₄⁺-N. Moisture content descent and ISFe content ascent improved the porosity of composting,

thus improving ORP and promoting the oxidation of NH₄⁺-N by *amoA*, simultaneously, along with the consumption of VS, DOC, TDN and NH₄⁺-N contents. Abundances of *nxrA* and *narG* on Day 0 were the maximum over the whole composting, and they were positive correlations with moisture content and contents of VS, DOC, NO₃⁻-N, NO₂⁻-N, seeming that the improvement of porosity and the utilization of NO₃⁻-N, NO₂⁻-N led to the decrement of *nxrA* and *narG*. Abundances of *nirK* and

norB had positive correlations with pH and NH_4^+ -N content, and had negative correlations with NO_3^- -N and NO_2^- -N contents. Importantly, it was found in Fig. 7b that main contributors to N_2O were NH_4^+ -N content, *norB* abundance and pH, implying that lower pH was conducive to retaining more NH_4^+ -N content. Additionally, NH_4^+ -N content and *norB* ascent enhanced N_2O emission.

3.6. Genes involved in methane metabolism

It is necessary to systematically ascertain alterations of typical methane-related functional genes (methanogenesis gene of *mcrA*, methane monooxygenase genes of *mmoX* and *pmoA*, methane dehydrogenase gene of *mxaF*) abundances, when discussing CH_4 generation from composting (He et al., 2019; Wang et al., 2022a; Wen et al., 2021). As shown in Fig. 6a, *mcrA* in three tests were all the highest of 8.16×10^7 , 9.16×10^7 and 7.26×10^7 copies/g on Day 0, there was no doubt that discharge of CH_4 concentrated in initial stage (Fig. 3b). Notedly, FeCl_2 enhanced *mcrA* abundance, while FeCl_3 had the opposite effect, corresponding to the phenomenon that FeCl_2 strengthened the first CH_4 release peak, yet FeCl_3 weakened the first CH_4 release peak on Day 1. As composting progressed, *mcrA* in Ctrl, FeII and FeIII sharply diminished to 1.21×10^7 , 5.59×10^6 and 3.22×10^6 copies/g on Day 10, suggesting that FeCl_2 and FeCl_3 both obviously weakened the second CH_4 release peak. Finally, *mcrA* almost disappeared in cooling period of each test. Contrary to alteration trend of *mcrA*, *mxaF* abundances stably increased from 1.42×10^7 to 4.40×10^7 copies/g of Ctrl, from 1.34×10^7 to 5.77×10^7 copies/g of FeII, and from 1.39×10^7 to 8.04×10^7 copies/g of FeIII over the entire composting (Fig. 6d).

Importantly, abundance of *pmoA* were all clearly higher than that of *mmoX* of each test in initial composting (Fig. 6b and c), suggesting that *pmoA* may play a more crucial role in methane oxidation. Additionally, *mmoX* and *pmoA* abundances presented the analogical variation tendency throughout the entire composting. Specifically, *mmoX* in Ctrl, FeII and FeIII significantly descended by 45.9 %, 37.9 % and 25.7 % ($p < 0.05$). Moreover, *pmoA* in Ctrl, FeII and FeIII apparently decreased by 76.3 %, 60.7 % and 51.9 % in the first 10 days ($p < 0.05$), respectively, meaning that initial composting was recalcitrant to *mmoX* and *pmoA* existences. Afterwards, with the improvement of aeration porosity in late composting stage, *mmoX* and *pmoA* of three tests separately elevated to 8.99×10^6 - 1.51×10^7 and 8.52×10^6 - 1.16×10^7 copies/g. It was worth noting that *mmoX*, *pmoA* and *mxaF* abundances of Ctrl were all much less than those of FeII and FeIII. Generally, the quite lower CH_4 emissions when adding FeCl_2 and FeCl_3 were possibly attributed to the elevation of *mmoX*, *pmoA* and *mxaF* abundances. More importantly, FeCl_3 had the more pronounced impact on CH_4 emission reduction because of *mcrA* decline in initial composting.

Similarly, correlations between four methane-related genes and environmental factors, and contributions of them to CH_4 production were separately obtained by PCA and RFA (Fig. 7c and d). Abundance of *mcrA* showed the positive relationship with moisture content, and negative correlations with ORP and ISFe content. On the contrary, abundances of *mmoX* and *pmoA* had negative relationships with moisture content, and positive correlations with ORP. High moisture content created the anaerobic environment with low ORP, thereby favorable to CH_4 release and avoidable to CH_4 oxidation. Moreover, abundances of four methane-related genes were all negative correlations with

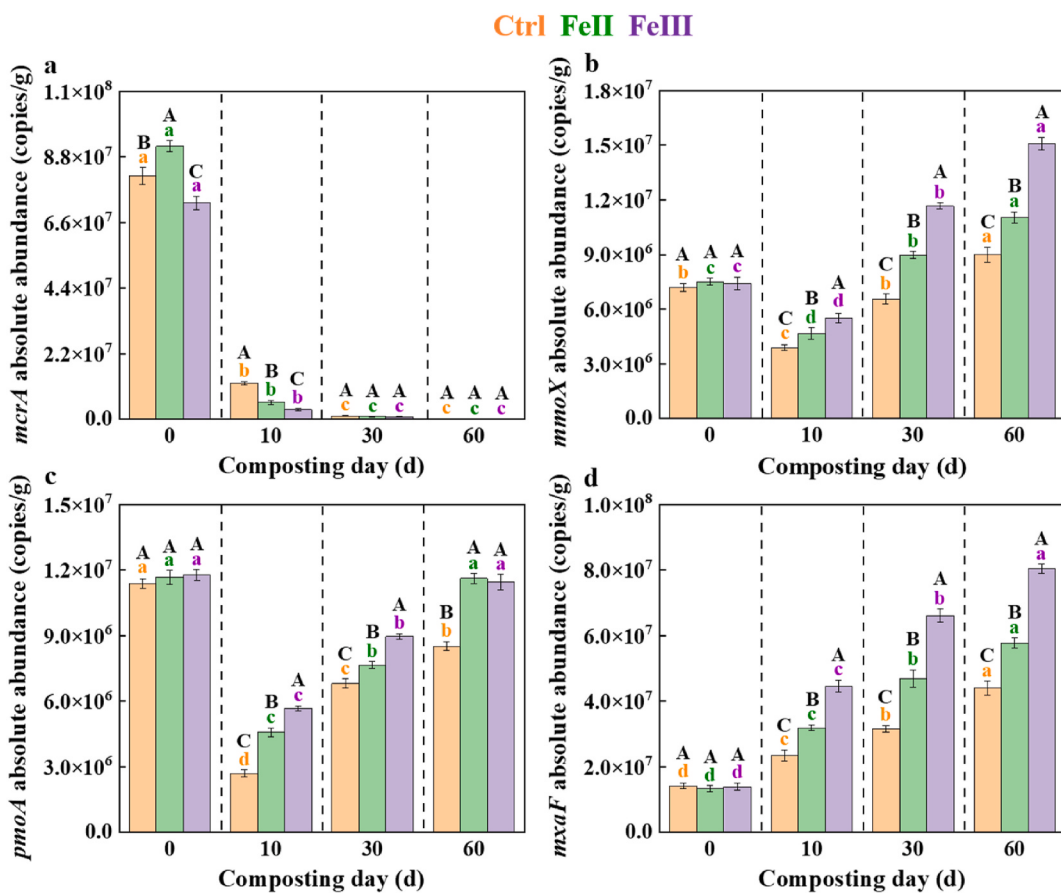


Fig. 6. Abundances of methane metabolism-related genes (*mcrA*, a; *mmoX*, b; *pmoA*, c; *mxaF*, d) in Ctrl, FeII and FeIII on Day 0, 10, 30 and 60 of 60 days swine manure composting, respectively. Ctrl, FeII and FeIII denoted composting of swine manure alone, and assisted-composting of swine manure with 3 % FeCl_2 and 3 % FeCl_3 , respectively. Capital letters above columns denoted significant differences at $p < 0.05$ among three treatments on the identical day. Lowercase letters in the same color above columns represented significant differences at $p < 0.05$ among composting days in the same treatment.

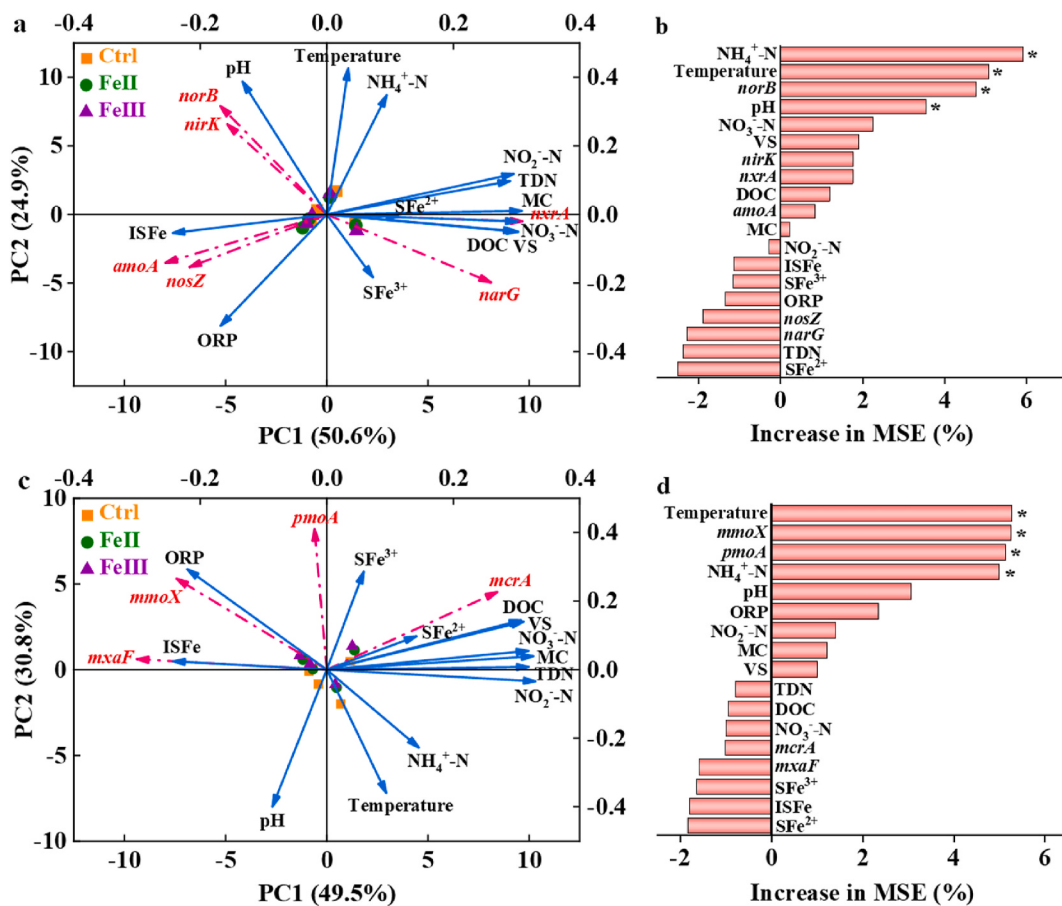


Fig. 7. Principal component analysis (PCA) between six nitrogen-related genes (*amoA*, *nxrA*, *narG*, *nirK*, *norB* and *nosZ*) absolute abundances and environmental factors (contents of soluble Fe²⁺, SFe²⁺; soluble Fe³⁺, SFe³⁺; insoluble Fe, ISFe; temperature; moisture content, MC; oxidation reduction potential, ORP; pH; contents of volatile solid, VS; dissolved organic carbon, DOC; total dissolved nitrogen, TDN; NH₄⁺-N; NO₃⁻-N; NO₂⁻-N) (a). Random forest analysis (RFA) on contributions of environmental factors and nitrogen-related genes to N₂O discharge (b). PCA between four methane-related genes (*mcrA*, *mmoX*, *pmoA* and *mxaf*) absolute abundances and environmental factors (c). RFA on contributions of environmental factors and methane-related genes to CH₄ discharge (d).

temperature, reflecting that high temperature prevented methane-related reactions. Notedly, *mmoX* and *pmoA* abundances presented positive relationships with ORP, showing that increment of them from Day 10 to Day 60 because of ORP enhancement. Interestingly, *mmoX* and *pmoA* abundances also exhibited a negative impact on NH₄⁺-N content, suggesting that the enrichment of NH₄⁺-N might prevent CH₄ oxidation. Furthermore, *mxaf* abundance was negatively correlated with contents of VS, DOC, TDN, and positively correlated with ORP, seeming that the dissipation carbon and nitrogen-containing OMs was helpful to the increment of *mxaf*. Importantly, dominant contributors to CH₄ were *mmoX*, *pmoA* genes, temperature and NH₄⁺-N content. As above-mentioned, CH₄ oxidation closely related to *mmoX* and *pmoA* genes. Moreover, high temperature and NH₄⁺-N content were adverse to CH₄ oxidation.

4. Conclusion

In summary, this research comprehensively studied effects of Fe on GHGs and NH₃ emissions from swine manure composting. Results demonstrated that soluble Fe salts were superior to insoluble Fe minerals on reducing GHGs total GWP. Additionally, Fe(III) salts were more effective on weakening CH₄, NH₃ and CO₂ emissions compared to Fe(II) salts. Specifically, FeCl₂ and FeCl₃ distinctly descended cumulative CH₄ emission by 35.7 % and 67.3 % ($p < 0.05$), and declined cumulative NH₃ emissions by 30.8 % and 37.3 % ($p < 0.05$), respectively. Importantly, FeCl₂ and FeCl₃ increased ORP, and mitigated *mmoX* and *pmoA* decrement in initial period, accounting for CH₄ release reduction. Moreover,

FeCl₂ and FeCl₃ both showed suppressive effects on methanogenic archaea of *Methanobrevibacter*. Although Fe(III) salts enhanced N₂O emission relative to Ctrl and Fe(II) salts, cumulative emission of N₂O was significantly lower than those of the other GHGs in the entire composting. FeCl₃ elevated NH₄⁺-N content, *nirK* and *norB* in initial period, which probably facilitated N₂O emission. Generally, this research made up the knowledge gap of how Fe(II) and Fe(III) affected GHGs and NH₃ emissions from composting, and proposed an environmental friendly alternative of FeCl₃ or FeCl₂-assisted composting to realize simultaneous CH₄ and NH₃ emissions reduction.

CRediT authorship contribution statement

Chen Zhang: Writing – original draft, Methodology, Formal analysis, Data curation, Conceptualization. **Xi Chen:** Writing – original draft, Methodology, Conceptualization. **Hailong Mao:** Methodology, Conceptualization. **Xiuming Zhang:** Methodology. **Ke Wang:** Writing – review & editing, Visualization, Investigation, Funding acquisition, Conceptualization. **Enhao Zhu:** Methodology. **Dan Yin:** Methodology. **Ruilun Zheng:** Writing – review & editing, Funding acquisition, Conceptualization. **Shijie You:** Investigation, Funding acquisition, Conceptualization.

Declaration of competing interest

The authors declare that they have no known competing financial interests or personal relationships that could have appeared to influence

the work reported in this paper.

Acknowledgements

This research was financially supported by National Natural Science Foundation of China (52170129 and U21A20161), Strategic Priority Research Program of the Chinese Academy of Sciences (XDC0230303), Chunyan Research Project of Heilongjiang Province (CYCX24022), Natural Science Foundation of Beijing Municipality (8232029), Project of National Engineering Research Center for Safe Sludge Disposal and Resource Recovery (2024A011), State Key Laboratory of Urban-rural Water Resource and Environment (Harbin Institute of Technology) (2025DX20).

Appendix A. Supplementary data

Supplementary data to this article can be found online at <https://doi.org/10.1016/j.jclepro.2025.146686>.

Data availability

Data will be made available on request.

References

- Cao, J.H., Li, C.J., Gao, X.D., Cai, Y.H., Song, X.L., Siddique, K.H.M., Zhao, X.N., 2023. Agricultural soil plastic as a hidden carbon source stimulates microbial activity and increases carbon dioxide emissions. *Resour. Conserv. Recy.* 198, 107151. <https://doi.org/10.1016/j.resconrec.2023.107151>.
- Cao, Y.B., Wang, X., Bai, Z.H., Chadwick, D., Misselbrook, T., Sommer, S.G., Qin, W., Ma, L., 2019. Mitigation of ammonia, nitrous oxide and methane emissions during solid waste composting with different additives: a meta-analysis. *J. Clean. Prod.* 235, 626–635. <https://doi.org/10.1016/j.jclepro.2019.06.288>.
- Chen, P.Z., Zheng, X.Q., Cheng, W.M., 2022. Biochar combined with ferrous sulfate reduces nitrogen and carbon losses during agricultural waste composting and enhances microbial diversity. *Process Saf. Environ. Prot.* 162, 531–542. <https://doi.org/10.1016/j.psep.2022.04.042>.
- Chen, Z.Q., Wu, Y.Q., Wen, Q.X., Ni, H.W., Chai, C.R., 2020. Effects of multiple antibiotics on greenhouse gas and ammonia emissions during swine manure composting. *Environ. Sci. Pollut. R.* 27 (7), 7289–7298. <https://doi.org/10.1007/s11356-019-07269-2>.
- Dai, X.X., Wang, X.J., Gu, J., Song, Z.L., Guo, H.H., Shi, M.L., Li, H.K., 2022. Mechanism associated with the positive effect of nanocellulose on nitrogen retention in a manure composting system. *J. Environ. Manage.* 316, 115308. <https://doi.org/10.1016/j.jenvman.2022.115308>.
- Du, X., Xing, R.Z., Lin, Y., Chen, M.L., Chen, Z., Zhou, S.G., 2024. Reduced greenhouse gas emission by reactive oxygen species during composting. *Bioresour. Technol.* 404, 130910. <https://doi.org/10.1016/j.biortech.2024.130910>.
- Fan, H.Y., Liao, J., Abass, O.K., Liu, L., Huang, X., Li, J., Tian, S.H., Liu, X.J., Xu, K.Q., Liu, C.X., 2021a. Concomitant management of solid and liquid swine manure via controlled co-composting: towards nutrients enrichment and wastewater recycling. *Resour. Conserv. Recy.* 168, 105308. <https://doi.org/10.1016/j.resconrec.2020.105308>.
- Fan, S.Y., Li, A.R., ter Heijne, A., Buisman, C.J.N., Chen, W.S., 2021b. Heat potential, generation, recovery and utilization from composting: a review. *Resour. Conserv. Recy.* 175, 105850. <https://doi.org/10.1016/j.resconrec.2021.105850>.
- Ge, J.Y., Huang, G.Q., Li, J.B., Han, L.J., 2018. Particle-scale visualization of the evolution of methanogens and methanotrophs and its correlation with CH₄ emissions during manure aerobic composting. *Waste Manag.* 78, 135–143. <https://doi.org/10.1016/j.wasman.2018.05.045>.
- Guo, H.H., Gu, J., Wang, X.J., Nasir, M., Yu, J., Lei, L.S., Wang, J., Zhao, W.Y., Dai, X.X., 2020a. Beneficial effects of bacterial agent/bentonite on nitrogen transformation and microbial community dynamics during aerobic composting of pig manure. *Bioresour. Technol.* 298, 122384. <https://doi.org/10.1016/j.biortech.2019.122384>.
- Guo, H.H., Gu, J., Wang, X.J., Yu, J., Nasir, M., Zhang, K.Y., Sun, W., 2020b. Microbial driven reduction of N₂O and NH₃ emissions during composting: effects of bamboo charcoal and bamboo vinegar. *J. Hazard. Mater.* 390, 121292. <https://doi.org/10.1016/j.jhazmat.2019.121292>.
- He, X.Q., Chen, L.J., Han, L.J., Liu, N., Cui, R.X., Yin, H.J., Huang, G.Q., 2017. Evaluation of biochar powder on oxygen supply efficiency and global warming potential during mainstream large-scale aerobic composting. *Bioresour. Technol.* 245 (PtA), 309–317. <https://doi.org/10.1016/j.biortech.2017.08.076>.
- He, X.Q., Han, L.J., Fu, B., Du, S.R., Liu, Y., Huang, G.Q., 2019. Effect and microbial reaction mechanism of rice straw biochar on pore methane production during mainstream large-scale aerobic composting in China. *J. Clean. Prod.* 215, 1223–1232. <https://doi.org/10.1016/j.jclepro.2019.01.159>.
- Hoang, H.G., Thuy, B.T.P., Lin, C., Vo, D.V.N., Tran, H.T., Bahari, M.B., Le, V.G., Vu, C.T., 2022. The nitrogen cycle and mitigation strategies for nitrogen loss during organic waste composting: a review. *Chemosphere* 300, 134514. <https://doi.org/10.1016/j.chemosphere.2022.134514>.
- Huang, Y.T., Yang, H.X., Li, K.C., Meng, Q.R., Wang, S.S., Wang, Y.W., Zhu, P.F., Niu, Q., Q., Yan, H.L., Li, X.L., Li, Q.L., 2022. Red mud conserved compost nitrogen by enhancing nitrogen fixation and inhibiting denitrification revealed via metagenomic analysis. *Bioresour. Technol.* 346, 126654. <https://doi.org/10.1016/j.biortech.2021.126654>.
- Jiang, J.S., Yu, D., Wang, Y., Zhang, X.D., Dong, W., Zhang, X.F., Guo, F.Q., Li, Y.B., Zhang, C.Y., Yan, G.X., 2021. Use of additives in composting informed by experience from agriculture: effects of nitrogen fertilizer synergists on gaseous nitrogen emissions and corresponding genes (*amoA* and *nirS*). *Bioresour. Technol.* 319, 124127. <https://doi.org/10.1016/j.biortech.2020.124127>.
- Jiang, T., Ma, X.G., Yang, J., Tang, Q., Yi, Z.G., Chen, M.X., Li, G.X., 2016. Effect of different struvite crystallization methods on gaseous emission and the comprehensive comparison during the composting. *Bioresour. Technol.* 217, 219–226. <https://doi.org/10.1016/j.biortech.2016.02.046>.
- Jiang, T., Schuchardt, F., Li, G.X., Guo, R., Zhao, Y.Q., 2011. Effect of C/N ratio, aeration rate and moisture content on ammonia and greenhouse gas emission during the composting. *J. Environ. Sci.* 23 (10), 1754–1760. [https://doi.org/10.1016/S1001-0742\(10\)60591-8](https://doi.org/10.1016/S1001-0742(10)60591-8).
- Li, K.Y., Xu, D., Zhang, L.M., Liu, W.J., Zhan, M., Su, Y.L., Wu, D., Xie, B., 2024. Integrated isotopic labeling analysis unveils precise proportions of ammonia emissions during composting. *J. Clean. Prod.* 450, 141799. <https://doi.org/10.1016/j.jclepro.2024.141799>.
- Liu, N.H., Liao, P., Zhang, J.C., Zhou, Y.Y., Luo, L., Huang, H.L., Zhang, L.H., 2020. Characteristics of denitrification genes and relevant enzyme activities in heavy-metal polluted soils remediated by biochar and compost. *Sci. Total Environ.* 739, 139987. <https://doi.org/10.1016/j.scitotenv.2020.139987>.
- Liu, Y., Tang, R.L., Li, L.Q., Zheng, G.N., Wang, J.N., Wang, G.Y., Bao, Z.Y., Yin, Z.M., Li, G.X., Yuan, J., 2023. A global meta-analysis of greenhouse gas emissions and carbon and nitrogen losses during livestock manure composting: influencing factors and mitigation strategies. *Sci. Total Environ.* 885, 163900. <https://doi.org/10.1016/j.scitotenv.2023.163900>.
- Liu, S.P., Lu, H., Wang, A., Chen, X.J., Yang, H.M., Liang, X.L., Sun, R., Wen, X.L., Li, Q.L., 2024. Sulfur and nitrogen co-metabolism during composting: a role of sodium sulfide in regulating microbial communities and functional genes. *J. Environ. Chem. Eng.* 12 (2), 112431. <https://doi.org/10.1016/j.jece.2024.112431>.
- Ma, R.N., Liu, Y., Wang, J.N., Li, D.Y., Qi, C.R., Li, G.X., Yuan, J., 2022. Effects of oxygen levels on maturity, humification, and odor emissions during chicken manure composting. *J. Clean. Prod.* 369, 133326. <https://doi.org/10.1016/j.jclepro.2022.133326>.
- Parodi, A., Gerrits, W.J.J., Van Loon, J.J.A., De Boer, I.J.M., Aarnink, A.J.A., Van Zanten, H.H.E., 2021. Black soldier fly reared on pig manure: bioconversion efficiencies, nutrients in the residual material, greenhouse gas and ammonia emissions. *Waste Manag.* 126, 674–683. <https://doi.org/10.1016/j.wasman.2021.04.001>.
- Qin, H.L., Wang, D., Xing, X.Y., Tang, Y.F., Wei, X.M., Chen, X.B., Zhang, W.Z., Chen, A.L., Li, L.L., Liu, Y., Zhu, B.L., 2021. A few key *nirk-* and *nosZ*-denitrifier taxa play a dominant role in moisture-enhanced N₂O emissions in acidic paddy soil. *Geoderma* 385, 114917. <https://doi.org/10.1016/j.geoderma.2020.114917>.
- Qu, J.S., Zhang, L.J., Zhang, X., Gao, L.H., Tian, Y.Q., 2020. Biochar combined with gypsum reduces both nitrogen and carbon losses during agricultural waste composting and enhances overall compost quality by regulating microbial activities and functions. *Bioresour. Technol.* 314, 123781. <https://doi.org/10.1016/j.biortech.2020.123781>.
- Ren, X.N., Wang, Q., Chen, X., He, Y.F., Li, R.H., Li, J., Zhang, Z.Q., 2021. Pathways and mechanisms of nitrogen transformation during co-composting of pig manure and diatomite. *Bioresour. Technol.* 329, 124914. <https://doi.org/10.1016/j.biortech.2021.124914>.
- Samuel, B.S., Hansen, E.E., Manchester, J.K., Coutinho, P.M., Henrissat, B., Fulton, R., Latreille, P., Kim, K., Wilson, R.K., Gordon, J.I., 2007. Genomic and metabolic adaptations of *Methanobrevibacter smithii* to the human gut. *Proc. Natl. Acad. Sci. USA* 104 (25), 10643–10648. <https://doi.org/10.1073/pnas.0704189104>.
- Shan, G.C., Li, W.G., Gao, Y.J., Tan, W.B., Xi, B.D., 2021. Additives for reducing nitrogen loss during composting: a review. *J. Clean. Prod.* 307, 127308. <https://doi.org/10.1016/j.jclepro.2021.127308>.
- Shen, X.L., Huang, G.Q., Yang, Z.L., Han, L.J., 2015. Compositional characteristics and energy potential of Chinese animal manure by type and as a whole. *Appl. Energy* 160, 108–119. <https://doi.org/10.1016/j.apenergy.2015.09.034>.
- Shen, Y.J., Ren, L.M., Li, G.X., Chen, T.B., Guo, R., 2011. Influence of aeration on CH₄, N₂O and NH₃ emissions during aerobic composting of a chicken manure and high C/N waste mixture. *Waste Manage. (Tucson, Ariz.)* 31 (1), 33–38. <https://doi.org/10.1016/j.wasman.2010.08.019>.
- Wang, J.N., Gao, X., Wang, G.Y., Liu, Y., Chang, J.L., Jiang, T., Li, G.X., Ma, R.N., Yang, Y., Yuan, J., 2024a. The enrichment of antibiotic resistance genes in swine manure compost was related to the bulking agent types. *Environ. Technol.* 36, 103765. <https://doi.org/10.1016/j.ennt.2024.103765>.
- Wang, J.X., Xie, H.F., Wu, J., He, W.J., Zhang, X., Huang, J.X., Feng, Y.F., Xue, L.H., 2024b. Fe/BC co-conditioners with environmental and economic benefits on composting: reduced NH₃ emissions and improved fertilizer quality. *Biochar* 6 (1), 4. <https://doi.org/10.1007/s42773-023-00295-x>.
- Wang, K., Du, M.F., Wang, Z., Liu, H.M., Zhao, Y., Wu, C.D., Tian, Y., 2022a. Effects of bulking agents on greenhouse gases and related genes in sludge composting. *Bioresour. Technol.* 344 (PtB), 126270. <https://doi.org/10.1016/j.biortech.2021.126270>.

- Wang, K., Li, W.G., Li, X.K., Ren, N.Q., 2015. Spatial nitrifications of microbial processes during composting of swine, cow and chicken manure. *Sci. Rep.* 5, 14932. <https://doi.org/10.1038/srep14932>.
- Wang, K., Wu, Y.Q., Li, W.G., Wu, C.D., Chen, Z.Q., 2018. Insight into effects of mature compost recycling on N₂O emission and denitrification genes in sludge composting. *Bioresour. Technol.* 251, 320–326. <https://doi.org/10.1016/j.biortech.2017.12.077>.
- Wang, X.Z., Liu, X., Wang, Z.Q., Sun, G.T., Li, J.M., 2022b. Greenhouse gas reduction and nitrogen conservation during manure composting by combining biochar with wood vinegar. *J. Environ. Manag.* 324, 116349. <https://doi.org/10.1016/j.jenvman.2022.116349>.
- Wang, Y.C., Akdeniz, N., Yi, S.Q., 2021. Biochar-amended poultry mortality composting to increase compost temperatures, reduce ammonia emissions, and decrease leachate's chemical oxygen demand. *Agric. Ecosyst. Environ.* 315, 107451. <https://doi.org/10.1016/j.agee.2021.107451>.
- Wen, P., Tang, J., Wang, Y.Q., Liu, X.M., Yu, Z., Zhou, S.G., 2021. Hyperthermophilic composting significantly decreases methane emissions: insights into the microbial mechanism. *Sci. Total Environ.* 784, 147179. <https://doi.org/10.1016/j.scitotenv.2021.147179>.
- Xie, J., Gu, J., Wang, X.J., Hu, T., Sun, W., Song, Z.L., Zhang, K.Y., Lei, L.S., Wang, J., Sun, Y.F., 2023. Response characteristics of denitrifying bacteria and denitrifying functional genes to woody peat during pig manure composting. *Bioresour. Technol.* 374, 128801. <https://doi.org/10.1016/j.biortech.2023.128801>.
- Xu, Z.C., Gao, X.Z., Li, G.X., Nghiem, L.D., Luo, W.H., Zhang, F.S., 2024. Microbial sources and sinks of nitrous oxide during organic waste composting. *Environ. Sci. Technol.* 58 (17), 7367–7379. <https://doi.org/10.1021/acs.est.3c10341>.
- Xue, S.D., Zhou, L.N., Zhong, M.Z., Awasthi, M.K., Mao, H., 2021. Bacterial agents affected bacterial community structure to mitigate greenhouse gas emissions during sewage sludge composting. *Bioresour. Technol.* 337, 125397. <https://doi.org/10.1016/j.biortech.2021.125397>.
- Yin, Q.D., Yang, S., Wang, Z.Z., Xing, L.Z., Wu, G.X., 2018. Clarifying electron transfer and metagenomic analysis of microbial community in the methane production process with the addition of ferroferric oxide. *Chem. Eng. J.* 333, 216–225. <https://doi.org/10.1016/j.cej.2017.09.160>.
- Zhang, K., Gan, R., Li, Y.X.Y., Chen, W., Ma, D.D., Chen, J., Luo, H.B., 2024. Effects of anaerobic oxidation of methane (AOM) driven by iron and manganese oxides on methane emissions in constructed wetlands and underlying mechanisms. *Chem. Eng. J.* 495, 153539. <https://doi.org/10.1016/j.cej.2024.153539>.
- Zhang, Z., Liu, D.H., Qiao, Y., Li, S.L., Chen, Y.F., Hu, C., 2021. Mitigation of carbon and nitrogen losses during pig manure composting: a meta-analysis. *Sci. Total Environ.* 783, 147103. <https://doi.org/10.1016/j.scitotenv.2021.147103>.
- Zhou, S.X., Li, Y., Jia, P.Y., Wang, X., Kong, F.L., Jiang, Z.X., 2022. The co-addition of biochar and manganese ore promotes nitrous oxide reduction but favors methane emission in sewage sludge composting. *J. Clean. Prod.* 339, 130759. <https://doi.org/10.1016/j.jclepro.2022.130759>.